

# The influence of biogeochemical conditions and level of model complexity when simulating cometabolic biodegradation in sorbent-water systems

Nathan W. Haws<sup>\*</sup>, Edward J. Bouwer, William P. Ball

*Department of Geography and Environmental Engineering, Johns Hopkins University, 3400 N. Charles Street, Baltimore, MD 21218-2686, USA*

Received 21 February 2005  
Available online 15 August 2005

## Abstract

Eighteen models with different levels of complexity for representing sorption, mass transfer, and biodegradation are used to simulate the biodegradation of toluene (primary substrate) and TCE (cometabolic substrate). The simulations are conducted for hypothetical completely mixed systems of various scenarios with regard to sorbent, microbial composition, and solute concentrations. The purpose of the suite of simulations is to investigate the sensitivity of different modeling approaches in simulating the bio-attenuation of co-existing solutes in sorbent-water systems. The sensitivity of results to the modeling approach depends on the biogeochemical conditions of the system. For example, the results are insensitive to the type of sorption model in systems with low sorption strength and slow biodegradation rates, and insensitive to the biodegradation rate model if mass transfer controlled. Differences among model results are generally greater when evaluated in terms of total mass removal rather than aqueous phase concentration reduction. The fate of the cometabolite is more sensitive to the proper consideration of co-solute effects than is the fate of the primary substrate. For a given system, graphical comparison of a characteristic mass transfer rate coefficient ( $\alpha_{mt}$ ) versus a characteristic biodegradation rate coefficient ( $\alpha_{bio}$ ) provides an indication of how sensitivity to the different processes may be expected to change with time and can guide the selection of an appropriate level of model complexity.

© 2005 Elsevier Ltd. All rights reserved.

*Keywords:* Bioavailability; Cometabolism; Model complexity; Sorption; Mass transfer; Biodegradation

## 1. Introduction

An ongoing difficulty in simulating the fate of contaminants in subsurface environments is that the modeled macro-scale phenomena are primarily governed by complex micro-scale processes that are hard to isolate and characterize in heterogeneous subsurface environments. For this reason, models developed using overly simplistic assumptions will fail under field conditions

that are outside the bound of their calibration [60]. These failures are often attributable to the small-scale and short-term conditions of laboratory experiments that do not adequately reflect longer-term rate phenomena [61], but also result from simplifications in the model formulations that do not sufficiently account for complex solute–soil, solute–microbial, and solute–solute interactions [32,65,69]. Practical constraints often prevent the full incorporation of all processes into a model, and there is an inherent conflict between the desire to constrain the model complexity (and associated uncertainty of model parameter values) with the need to more mechanistically model complex processes [12,13,42].

<sup>\*</sup> Corresponding author. Tel.: +1 410 516 4255.

E-mail addresses: [nhaws@jhu.edu](mailto:nhaws@jhu.edu) (N.W. Haws), [ebouwer@jhu.edu](mailto:ebouwer@jhu.edu) (E.J. Bouwer), [bball@jhu.edu](mailto:bball@jhu.edu) (W.P. Ball).

One area in which past model simplifications have been inadequate (and where laboratory data have provided new insight) is in regard to sorption and the related issues of mass transfer (e.g., desorption). Recent studies have underscored the need to better delineate and represent complex sorption mechanisms and desorption/diffusion processes. For example, research has shown that using linear isotherms as a convenient approximation for nonlinear sorption can lead to large errors in predicting aqueous concentrations (e.g., [16,61,68]). Other work has shown that the commonly used first-order rate model for simulating desorption and intraparticle mass transfer oversimplifies sorption and desorption dynamics and can lead to large errors after long times of desorption or under scenarios that involve time-variant boundary conditions external to the sorbent particle (e.g., [37,38,51,59,61,83]). Even highly mechanistic pore diffusion models are often inaccurate for natural sorbents and porous media because they can never precisely account for inherent heterogeneities in particle shapes, sizes, sorption capacities, sorbent-phase pore volumes and internal structures (e.g., [10,22,46,57]). Co-existing solutes also can affect both sorption and mass transfer by competing for sorption sites (e.g., [36,52,62,79]).

Given such complexities, increased sophistication has been incorporated into numerical models to describe pollutant fate and remediation. For example, improved sorption isotherm models are available to more mechanistically describe sorption nonlinearity by more distinctly accounting for the simultaneous absorption into natural organic matter and adsorption onto “harder” substances [2,43,44,77,78,80,81], and models have also been developed to consider competitive sorption in multi-solute systems (e.g., [27,54,62]). Some recently developed models for mass transfer explicitly account for diffusion in particles of different sizes, geometries, and internal porosities [10,46], and others consider particle heterogeneities using multiple rate constants (e.g., [24,45,73]), including stochastic approaches with statistical distributions of rate or combinations of rate and sorption capacity (e.g., [22,39,57]).

Biodegradation kinetics are also modeled with various approaches. Although first-order models offer simplifications valuable for model construction and interpretation, biodegradation models are also available for more mechanistically representing concepts of enzyme saturation and biomass growth. These include not only the classical Monod equation [21,49,55], but also modifications to the Monod equation that can account for the formation of toxic degradation products (e.g., [28,30]), co-solute inhibition, and cometabolism (e.g., [6,26]).

The increased sophistication of sorption, diffusion, and biodegradation models has led to a greater ability to predict and simulate solute fate in many well-defined laboratory experiments. For poorly characterized sys-

tems, however, a drawback to increased model sophistication is that more complex models invariably have a greater number of parameters, not all of which can be independently determined using currently available methods [70]. In such cases, the better fit to experimental data may be only a result of an increase in the degrees of freedom and may not truly reflect a more mechanistic representation of the governing processes [33,34,45]. Thus, when a detailed characterization of biogeochemical properties is impractical or infeasible, what is likely a more mechanistic representation is compromised by assuming a simpler model that can be more easily parameterized and implemented. Given that all models can never be fully mechanistic for complex and heterogeneous media, the choice of an “appropriate” model is often unclear. A general rule (sometimes referred to as Occam’s Razor) is that the most appropriate model for a given situation is that which uses as few unspecified parameters as possible to describe the principal outcomes of concern with reasonable accuracy. Use of such a model will minimize the possibility of nonunique parameters and increase the likelihood that the parameters are appropriately descriptive for the system at hand [42]. In this context, exploring the sensitivity of a model’s results to various simplifying assumptions can offer insight into model selection.

This paper explores model sensitivity for co-solute systems as influenced by solute concentration, sorption, mass transfer, and cometabolic biodegradation in order to provide insight on the level of modeling complexity that is needed for different system conditions. Several models with hierarchical levels of complexity in their process representations are used to simulate cometabolic biodegradation in some selected hypothetical, completely mixed domains that represent volume elements of water-saturated porous media. Toluene and TCE are used as model contaminants for the primary (growth) and cometabolic (nongrowth) substrates. Although a comprehensive analysis of all models and environmental scenarios is obviously not possible, the case studies presented do illustrate how different combinations of biogeochemical factors affect model sensitivity in well-mixed systems that include cometabolic biodegradation.

## 2. Concepts and methods

### 2.1. Model development

The assumed modeling domain is a finite-volume, completely mixed, soil–water system in which the solute mass changes over time can be related by the following:

$$\frac{\partial M_T(t)}{\partial t} = \frac{\partial M_w(t)}{\partial t} + \frac{\partial M_s(t)}{\partial t} \quad (1)$$

where  $M$  ( $\mu\text{mol}$ ) is the solute mass,  $t$  ( $d$ ) is time, and the subscripts T, w, and s, denote the total domain, bulk aqueous phase, and solid phase (sorbed to particle solids or in the aqueous phase of an intraparticle region). The solute mass balance is further defined by

$$\frac{\partial M_w(t)}{\partial t} = V_w \frac{\partial C_w(t)}{\partial t} - r_{\text{bio}}(t) \cdot V_w \quad (2)$$

$$\frac{\partial M_s(t)}{\partial t} = m_T \frac{\partial C_s(t)}{\partial t} \quad (3)$$

where  $C_w$  ( $\mu\text{mol/L}$ ) is the solute concentration in the bulk aqueous phase (aqueous phase external to solids),  $C_s$  ( $\mu\text{mol/kg}$ ) is the solute concentration in the solid phase,  $V_w$  (L) is the volume of water in the bulk aqueous phase,  $m_T$  (kg) is the total mass of the solids, and  $r_{\text{bio}}$  ( $\mu\text{mol/d}$ ) is the biodegradation rate. Note that Eq. (2) is a reflection of the fact that biodegradation is often found to occur only in the bulk aqueous phase such that the sequestration of solutes by solids limits the accessibility, or bioavailability, of solutes to biodegradation (e.g., [11,32,50,65,66,71]).

Using the conceptual framework given above, numerical models were constructed based on different representations of mass transfer, sorption, and biodegradation. These components are discussed below.

### 2.1.1. Desorption and mass transfer

Desorption and mass transfer kinetics are simulated in this work using one of three models: equilibrium (E), simplistic (S), or diffusion (D). The equilibrium model assumes instantaneous sorption and desorption such that the solid phase concentration is at local equilibrium with the bulk aqueous phase. The following equation then describes the mass balance in the solid (sorbed) phase:

$$\frac{\partial C_s}{\partial t} = \frac{dC_s}{dC_w} \frac{\partial C_w}{\partial t} \quad (4)$$

where the partitioning coefficient,  $\frac{dC_s}{dC_w}$ , can be obtained from the sorption isotherm.

The simplest model for describing rates of sorption or desorption (mass transfer rates) is a first-order approach that partitions the domain into two regions: Region 1, a macroporosity region (porosity external to sorbent particles), and Region 2, a microporosity region (porosity internal to the sorbent particles). Microbes cannot access the micropores so that biodegradation occurs only in the aqueous solution of Region 1 (e.g., [11,32,50,65,66,71]). Concentrations within each region are completely mixed and at local equilibrium with the sorbed phase; however, solute mass exchange between the two regions is rate-limited and governed by the concentration difference between each region and a simple first-order mass transfer coefficient,  $\alpha_p$  [ $\text{s}^{-1}$ ]. The mass balance in Region 2 is then given by Eq. (5):

$$\varepsilon_i \frac{\partial C_2}{\partial t} + \rho_g \frac{\partial S_2}{\partial t} = \alpha_p (C_1 - C_2) \quad (5)$$

where  $\varepsilon_i$  [ $\text{cm}^3/\text{cm}^3$ ] is the internal grain porosity (i.e., the porosity of Region 2),  $\rho_g$  [ $\text{g}/\text{cm}^3$ ] is the apparent grain density (i.e., the bulk density within Region 2),  $C$  ( $\mu\text{mol/L}$ ) is the aqueous phase concentration,  $S$  ( $\mu\text{mol/kg}$ ) is the sorbed phase concentration, and subscripts 1 and 2 denote Region 1 and Region 2, respectively. With this conceptualization,  $V_w$  is distinguished from the total aqueous volume,  $V_T$ , by

$$V_w = V_T - \frac{m_T \varepsilon_i}{\rho_g} \quad (6)$$

and the definition of  $C_s$  becomes

$$C_s(t) = S_1(t) + S_2(t) + \frac{\varepsilon_i}{\rho_g} C_2(t) \quad (7)$$

The first-order model (referred to as the “simplistic” model to avoid ambiguity with subsequent uses of the term “first-order”) is representative of linear driving force models [20,76] that are commonly used to approximate more complicated mass exchange processes between the bulk aqueous phase and the solid phase [82].

The diffusion model for desorption/mass transfer is also a two-region mass transfer model, but solute in Region 2 is not assumed to be completely mixed. Rather, solute movement in Region 2 is controlled by Fickian diffusion. For assumptions of a spherical Region 2 domain and diffusion only in water, the movement of solute in Region 2 can be described by the following equation:

$$\varepsilon \frac{\partial C_2}{\partial t} + \rho \frac{\partial S_2}{\partial t} = \frac{\varepsilon D_p}{r^2} \frac{\partial}{\partial r} \left( r^2 \frac{\partial C_2}{\partial r} \right) \quad (8)$$

where  $r$  (cm) is the particle’s radial coordinate, and  $D_p$  ( $\text{cm}^2/\text{day}$ ) is the pore diffusion coefficient [9]. For use with Eq. (7), sorbed and aqueous concentrations in Region 2 must be averaged across the intraparticle region (Region 2) of radius  $a$  (cm):

$$\bar{C}_2(t) = \frac{3}{a^3} \int_0^a C_2(r, t) r^2 dr \quad (9a)$$

$$\bar{S}_2(t) = \frac{3}{a^3} \int_0^a S_2(r, t) r^2 dr \quad (9b)$$

Mass transfer between the particle surface and the bulk aqueous phase is assumed to be rapid compared to intraparticle diffusion rates so that the aqueous concentration at the particle surface equals the bulk aqueous concentration:

$$C_2(r = a, t) = C_1(t) \quad (10)$$

Sorbed concentrations in each region are related to their respective aqueous phase concentration through an appropriate sorption isotherm:

$$S_1(t) = f \frac{dC_s}{dC_w} C_1(t) \quad (11a)$$

and

$$S_2(t) = (1 - f) \frac{dC_s}{dC_w} C_2(t) \quad (11b)$$

where  $f$  is the fraction of sorption sites attributed to Region 1.

Although the above model is vastly simplified by assuming a single geometry and size for Region 2, it is nonetheless an arguably more mechanistic representation of intraparticle mass transfer than the simple first-order model because it allows an accounting of time-variant concentration gradients within the sorbed phase. In this work, the diffusion model is used as a hypothetical construct that might represent either the retarded pore diffusion model or other, more complex, rate models that assume multiple first-order rate constants to characterize mass transfer (e.g., [22,45,57,73]).

### 2.1.2. Equilibrium sorption isotherms

Equilibrium sorption is also represented by one of three different models: linear (L), nonlinear (N), or nonlinear-competitive (Nc). Partitioning in the nonlinear model is represented by the Freundlich isotherm:

$$\frac{dC_s}{dC_w} = nK_f C_w^{n-1} \quad (12)$$

where  $K_f$  ((L/kg) <sup>$n$</sup> ) and  $n$  (–) are coefficients of the isotherm. For the linear sorption model,  $n = 1$  and  $K_f$  reduces to the linear solid–water partition coefficient,  $K_d$  (L/kg).

The nonlinear-competitive model accounts for the effects of solute competition for sorption sites in multi-component solutions using the Ideal Adsorbed Solution Theory (IAST). For a system with two solutes, the IAST sorption isotherm is derived from the individual Freundlich isotherm parameters for each of two solutes,  $i$  and  $j$  [27,54,58]:

$$C^i = \left( \frac{S^i}{S^i + S^j} \right) \left[ \frac{S^i + S^j \left( \frac{n^j}{n^i} \right)}{K_f^i} \right]^{\frac{1}{n^i}} \quad (13)$$

### 2.1.3. Biodegradation

Biodegradation is likewise simulated using one of three alternative models: first-order (F), Monod (M), or Monod with inhibition and cometabolism (Mc). The first-order model represents the biodegradation rate,  $r_{\text{bio}}$ , with a first-order rate constant,  $k_1$  (1/d):

$$r_{\text{bio}} = k_1 C_w \quad (14)$$

The Monod biodegradation model accounts for the interdependence of the substrate utilization rate and the biomass growth rate,  $r_x$  (mg<sub>x</sub>/L d):

$$r_{\text{bio}} = \frac{k_m X C_w}{K_s + C_w} \quad (15)$$

$$r_x = \frac{dX}{dt} = Yr_{\text{bio}} - bX \quad (16)$$

where  $X$  (mg<sub>x</sub>/L) is the biomass density,  $Y$  (mg<sub>x</sub>/μmol) is the yield coefficient,  $k_m$  (μmol/mg<sub>x</sub> d) is the maximum rate of substrate utilization,  $K_s$  (μmol/L) is the half-saturation constant, and  $b$  (1/d) is a first-order biomass death rate.

Models for dual-substrate inhibition and cometabolism modify the Monod equation to account for co-solute inhibition, degradation rate enhancement of a primary growth substrate (superscript g) on a cometabolite (superscript c), and increased biomass decay due to toxic product formation from the degradation of the cometabolite [3–6,21,26,49]. Kinetic expressions show the interrelationship between primary growth substrate and cometabolite biodegradation:

$$r_{\text{bio}}^g = \frac{k_m^g X C_w^g}{K_s^g \left( 1 + \frac{C_w^c}{K_i^c} \right) + C_w^g} \quad (17)$$

$$r_{\text{bio}}^c = (T_y r_{\text{bio}}^g + k_m^c X) \cdot \left[ \frac{C_w^c}{K_s^c \left( 1 + \frac{C_w^g}{K_i^g} \right) + C_w^c} \right] \quad (18)$$

where  $K_i$  (μmol/L) is the competitive inhibition coefficient and  $T_y$  (μmol<sup>c</sup>/μmol<sup>g</sup>) is the transformation yield for the biodegradation rate enhancement of the cometabolite due to the degradation of the primary growth substrate. The negative effects on the microbial population of toxic product formation resulting from the transformation of the cometabolite are included in the  $r_x$  term using a transformation capacity,  $T_c$  (μmol/mg<sub>x</sub>):

$$r_x = Yr_{\text{bio}}^g - bX - \frac{r_{\text{bio}}^c}{T_c} \quad (19)$$

The three representations each for the mass transfer, sorption, and biodegradation components yield a possibility of 27 model combinations. Of these 27 combinations, 18 are used in this study. The 18 models range from the simplest model representation of equilibrium linear sorption with first-order biodegradation to a more complex model with nonlinear-competitive sorption, diffusive mass transfer and cometabolic biodegradation. These models were selected from the possible 27 as follows: Only two of the possible nine equilibrium models were chosen, the E–L–F model (simplest) and E–Nc–Mc (most complex of the equilibrium models), since the equilibrium models are the most simplistic conceptualization. All other model formulations were used except the Monod biodegradation formulation for nonlinear and competitive sorption with either the simple mass transfer or diffusion mass transfer models (S–Nc–M and D–Nc–M). These two model formulations were not included as they offered little new information compared to their counterpart linear and noncompetitive formulations (S–N–M and D–N–M). Fig. 1 depicts the model combinations selected for this study along with the abbreviations that are used to identify each.

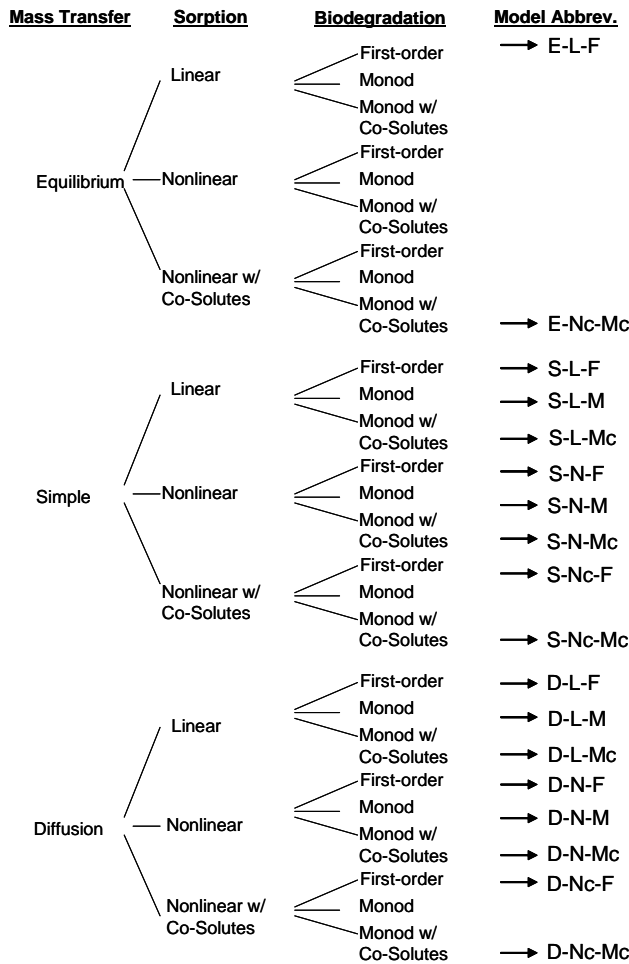


Fig. 1. Combinations of model representations for mass transfer, sorption, and biodegradation. Abbreviations are given for the model combinations used in this study.

The diffusion mass transfer model with linear and nonlinear sorption is taken from NNpore numerical code of Young [82] and Young and Ball [84] which was also adapted and applied by Sabbah et al. [61]. Aqueous and sorbed phase concentrations in the NNpore model are solved using a predictor–corrector approach [84] and the intraparticle diffusion is computed using a tri-diagonal matrix algorithm [66,82] with a Crank–Nicholson finite difference numerical procedure [25]. This base model is further extended here to simultaneously track two chemical species. If the competitive sorption model formulation is chosen, the aqueous and sorbed concentrations of the two chemicals are solved iteratively using IAST (Eq. (13)). The mass biodegraded for each time step is computed after solving for aqueous and sorbed phase concentrations using the first-order, Monod, or Monod with co-solutes model, depending on the formulation selected by the user. The simple mass transfer model uses the same solution procedure as the diffusion mass transfer model except that aqueous concentrations in Region 2 are completely mixed at each

time step. The equilibrium formulation was derived from the diffusion model by specifying a mass transfer rate fast enough to mimic equilibrium conditions at each time step.

The initial distribution of aqueous and sorbed concentrations in Region 1 and Region 2 are set at the equilibrium condition as given by the sorption isotherm for the respective solute and soil type scenario. The boundary condition between Region 1 and Region 2 is given by Eq. (10).

### 2.2. Hypothetical case studies and model parameterization

All simulations are conducted for a hypothetical, 1-L batch system containing toluene and trichloroethylene (TCE). These solutes were chosen because of their environmental relevance, because they function as exemplary cometabolic substrates with toluene as the primary growth substrate and TCE as the nongrowth cometabolite, and because of the availability of numerous previously reported biodegradation rate parameters for the combined system. In particular, as reviewed by Alvarez-Cohen and Speitel [6], a number of researchers have documented that TCE will be cometabolically degraded with toluene by pure cultures (*Pseudomonas bac-*teria) and mixed cultures.

Hypothetical case studies explore combinations of different soil types (high and low sorption strength in combination with slow and fast mass transfer rates), biodegradation rates (fast and slow), and initial mass loadings (high and low). In all scenarios, the total soil mass and total water volume are assumed to be 1.62 kg and 0.38 L, respectively, which gives a soil–water ratio ( $R_{s/w}$ ) of 4.3. This value is typical of many saturated aquifers, but higher than what could be easily studied in a batch laboratory system. Other system properties general to all scenarios are the apparent grain density,  $\rho_g = 2.62 \text{ kg/L}$ , and the intraparticle porosity,  $\epsilon_i = 0.018$  [84]. The case-specific parameters are provided below.

#### 2.2.1. Sorption and mass transfer parameters

The sorption and mass transfer parameters are selected to be characteristic of two endpoint conditions: (1) a scenario with relatively weak sorption and rapid mass transfer (labeled “Type 1 soil”) and (2) a scenario with relatively strong sorption and slow mass transfer (labeled “Type 2 soil”). Parameters for the Type 1 soil are based on pulverized sand from the Borden aquifer (Borden, Ontario) with an organic carbon fraction,  $f_{oc} = 0.00023$  and a mean particle diameter between 250  $\mu\text{m}$  and 420  $\mu\text{m}$  [8,9]. For this material, Harmon and Roberts [40] measured a perchloroethene (PCE) diffusion rate coefficient ( $D_p/a^2$ ) of  $0.74 \text{ d}^{-1}$ . The diffusion coefficient for PCE is translated into  $D_p/a^2$  values for

toluene and TCE using the Wilke–Chang proportionality:

$$\frac{D_p}{a^2}(\text{toluene, TCE}) = \frac{D_p}{a^2}(\text{PCE}) \frac{D_m(\text{toluene, TCE})}{D_m(\text{PCE})} \quad (20)$$

where  $D_m$  is the solute diffusion coefficient in water. The  $D_m$  values of PCE, toluene and TCE are estimated from the method of Hayduk and Laudie [41] as 0.75 cm<sup>2</sup>/d, 0.73 cm<sup>2</sup>/d, and 0.81 cm<sup>2</sup>/d, respectively. The corresponding diffusion rate parameters for the Type 1 soil are 0.7 d<sup>-1</sup> for toluene and 0.8 d<sup>-1</sup> for TCE.

Although Ball and Roberts [8] found PCE sorption with Borden sand to be higher than predicted by common regressions with organic carbon content, this work assumes that conventional organic carbon relationships are adequate to describe sorption equilibrium parameters. For the linear sorption models,  $K_d$  is estimated from the following relationship:

$$K_d = f_{oc} K_{oc} \quad (21)$$

where  $K_{oc}$  (L/kg) is the soil–water partition coefficient normalized to organic carbon. The  $K_{oc}$  value for toluene, 150 L/kg, is taken directly from values reported by EPA [31]. The  $K_{oc}$  value for TCE, 104 L/kg, is estimated with [47,64]:

$$\log K_{oc} = 0.95 \log K_{ow} - 0.2 \quad (22)$$

where the log value of the octanol–water partition coefficient,  $\log K_{ow}$ , of 2.32 is taken from the averages of several literature values assembled by Schaerlaekens et al. [64]. For the nonlinear sorption model, an  $n$  value of 0.6 was selected. The Freundlich  $K_f$  parameter in the Type 1 soil and Type 2 soil scenarios were derived by matching the initial equilibrium concentrations of linear and nonlinear sorption isotherms. The isotherm matching was done for both the high initial mass loading case and the low initial mass loading case (see Section 2.2.3). Because the “matched”  $K_f$  is dependent on concentration, this double  $K_f$  matching effectively created four soils (two of which are “Type 1” for high and low mass loading and two of which are “Type 2” for high and low mass loading). This is done so that comparisons can be made for situations with similar amounts of sorption at the initial condition of contamination.

The first-order mass transfer terms for the models with the simplistic (first-order) mass transfer representation are related to the asymptotic mass transfer rate of the diffusion model with a geometry specific shape-factor,  $\beta$  (–) (e.g., [9,56,74,75]):

$$\alpha_p \approx \beta \frac{D_p}{a^2} \quad (23)$$

where  $\beta$  is approximately 15 for spherical particles. Using Eq. (23), the equivalent  $\alpha_p$  values for the Type 1 soil are 10.5 d<sup>-1</sup> for toluene and 12 d<sup>-1</sup> for TCE.

The Type 2 soil is derived from the Type 1 soil by increasing the sorption strength and decreasing the mass transfer rate. For the Type 2 soil, the  $f_{oc}$  is increased by a factor of 100 and the  $D_p/a^2$  value is decreased by a factor of 10 from that of the Type 1 soil. (This might thus represent larger grained material of greater sorption capacity.) Then, the methods of estimating the values for sorption and mass transfer parameters in the Type 2 soil were similar to those used to estimate the parameter values for the Type 1 soil. The  $f_{oc}$  and  $D_p/a^2$  for the Type 2 soil, as well as the small  $n$  value of 0.6 for the nonlinear sorption isotherms, were selected in order to represent domains with high sorption, slow mass transfer, and/or strong nonlinear sorption effects. Although the differences between the sorption and mass transfer parameters of the Type 1 and Type 2 soils were large, all parameters are not unrealistic of some soil–water environments (e.g., [23,40,62]), and the two soil types represent endpoints of environmentally relevant scenarios. It should be noted that by correlating low sorption with rapid mass transfer (and vice versa), the apparent diffusion rates ( $D_a/a^2$ ), which are reduced by the sorption retardation factor in Region 2, vary by nearly 3 orders of magnitude among the two soils scenarios in comparison to the factor of 10 difference of the  $D_p/a^2$  values. (Table 1 reports both  $D_p/a^2$  and  $D_a/a^2$  values.)

It is also important to note that the two soil type scenarios do not account for all possible sorption and mass transfer combinations. Since soil–water partitioning retards the apparent pore diffusion rate, strong sorption is commonly related to slow mass transfer rate (and vice versa); however,  $D_p$  is an intrinsic rate which depends only on particle size, internal porosity, and tortuosity (unlike the apparent diffusion rate,  $D_a$ , which also depends on the local retardation factor). Thus, situations with strong sorption and rapid mass transfer or weak sorption and slow mass transfer are also possible (For example, fine particles with high organic carbon contents such as soots and chars). Consequently, two other soil types are investigated: Type 1-r and Type 2-r. The Type 1-r soil has the same sorption parameters as the original Type 1 soil, but a  $D_p/a^2$  value that gives a  $D_a/a^2$  that is equivalent to the  $D_a/a^2$  of the original Type 2 soil. Likewise, the Type 2-r soil has sorption parameters identical to the Type 2 soil and a  $D_a/a^2$  that matches the Type 1 soil. Only the high  $M_0$  and slow biodegradation rate scenarios are simulated for the Type 1-r and Type 2-r soils.

### 2.2.2. Biodegradation parameters

As with the sorption and mass transfer parameters, two scenarios of biodegradation rates are selected (“fast” and “slow”) with an objective to span an appropriate range of realistic biodegradation rates. Biodegradation rate parameter values for the single and cometabolic Monod models for toluene and TCE are

Table 1

Equilibrium sorption partition coefficients and mass transfer rate coefficients used for toluene and TCE in the simulations with the Type 1 soil and the Type 2 soil

	Toluene		TCE	
	Type 1	Type 2	Type 1	Type 2
$D_p/a^2$ (d <sup>-1</sup> )	0.7	0.07	0.8	0.08
$D_a/a^2$ (d <sup>-1</sup> ) <sup>a</sup>	0.13	0.00016	0.20	0.00027
$\alpha_p$ (d <sup>-1</sup> )	10.5	1.05	12	1.2
$\alpha_a$ (d <sup>-1</sup> ) <sup>a</sup>	2.0	0.0024	3.0	0.0041
$K_d$ (L kg <sup>-1</sup> )	0.035	3.5	0.024	2.4
$K_f$ ((L kg <sup>-1</sup> ) <sup>n</sup> )	<i>0.77</i> (0.12)	27 (4.3)	<i>0.21</i> (0.034)	8.5 (1.3)
$n$ (–)	0.6	0.6	0.6	0.6

$K_f$  values listed in italics are for the high initial mass loading cases and values listed in parentheses are for the low initial mass loading cases.

<sup>a</sup> The apparent mass transfer rates are reported for the linear sorption model. The actual apparent mass transfer rates for the nonlinear sorption model depend on the solute concentrations.

Table 2

Biodegradation parameters used for “fast” and “slow” biodegradation rate scenarios

	Toluene <sup>a</sup>		TCE <sup>b</sup>	
	Fast (pure cultures)	Slow (mixed cultures)	Fast (pure cultures)	Slow (mixed cultures)
$k_m$ (μmol mg cells <sup>-1</sup> d <sup>-1</sup> )	200	130	8	2
$K_s$ (μmol L <sup>-1</sup> )	30	100	10	30
$K_i$ (μmol L <sup>-1</sup> )	10	10	30	30
$Y$ (mg cells μmol <sup>-1</sup> )	0.05	0.03	n.a.	n.a.
$T_y$ (μmol μmol <sup>-1</sup> )	n.a.	n.a.	0.09	0.05
$T_c$ (μmol mg cells <sup>-1</sup> )	n.a.	n.a.	8.3	8.3
$k_1$ (d <sup>-1</sup> )	33	6.5	4.0	0.33

<sup>a</sup> Based on average of values reported in [1,7,17,18,21,48,67].

<sup>b</sup> Based on average of values reported in [4,6,17,29,67].

estimated from values compiled by [1,6,7,67], as well as other individual studies (see footnotes of Table 2). Because observed field-scale biodegradation rates are influenced by other concurrent processes [7,72], biodegradation rate parameters are selected based on data from studies conducted in batch system with no solids. Also, because TCE cometabolism rates tend to vary widely with the accompanying growth substrate, the TCE biodegradation rate parameter values are taken only from studies that used toluene or phenol as the primary growth substrate. Biodegradation rates in studies using pure-strain microbial cultures are generally greater than those reported for studies using mixed microbial cultures; therefore, biodegradation rate parameter values for the “fast” biodegradation rate scenarios are based on the average values for studies using pure cultures, and parameter values for the “slow” biodegradation rate scenario are based on the average values for studies using the mixed cultures. The transformation capacity,  $T_c$ , is kept at a relatively high value (8.3 μmol/μmol) for both the “fast” and “slow” rates so that the  $T_c$  term had an effect on, but did not dominate the biodegradation rate. Values for the  $K_i$  parameter are not reported in most studies. Therefore, the value of the “fast”  $K_s$  is used for both the “fast” and “slow”  $K_i$  values. The validity of substituting  $K_s$  values for  $K_i$

values is still under debate [6]; however, a lack of available  $K_i$  values necessitates this assumption. For each simulation, the initial biomass concentration,  $X_0$ , is set at 5 mg/L, which is typical of batch studies (e.g., [1,53,63]).

The values for  $k_1$  in the first-order biodegradation model are estimated from the Monod biodegradation parameters using

$$k_1^g \simeq \frac{k_m^g X_0}{K_s^g} \quad \text{and} \quad k_1^c \simeq \frac{k_m^c X_0}{K_s^c} \quad (24)$$

The parameter values for all biodegradation models are reported in Table 2.

### 2.2.3. Initial mass loading

The initial solute concentrations also affect the significance of co-solute competition and the sensitivity of assuming first-order biodegradation versus using Monod kinetics. In this study, two cases of mass loading (initial solute concentration) are considered: one with a high initial contaminant mass ( $M_0$ ) and one with a low  $M_0$ . For TCE, the high  $M_0$  was 100 μmol and the low  $M_0$  was 1 μmol. The  $M_0$  for toluene is set at 10 times the  $M_0$  for TCE, which is consistent with TCE bioremediation studies in which toluene is supplied in excess of TCE [35]. The  $M_0$  values are selected to provide initial

high/low concentrations that bound typical values used in biodegradation and bioremediation studies (e.g., [6,53,63]). The initial solute concentration distributions between the aqueous and sorbed phases are set at the equilibrium partitioning value based on their sorption isotherms. Recall that using a high and a low  $M_0$  means that in the isotherm matching to determine the  $K_f$  value of the Freundlich isotherms that essentially four soil types are created because of the concentration dependence of nonlinear sorption (see Section 2.2.1).

The different scenarios for sorption, mass transfer rates, biodegradation rates, and initial mass loading combine to give eight case studies for each of the eighteen models considered. The results of each model are evaluated based on the relative mass remaining in the total domain ( $M/M_0$ ) and on the relative concentration in the bulk aqueous solution ( $C_w/C_{w0}$ ). The evaluation based on  $M/M_0$  takes the perspective of a mass-based compliance criterion that requires a rigorous extraction from both solid and aqueous phase. By contrast, the evaluation based on  $C_w/C_{w0}$  corresponds to a compliance criterion where only the aqueous phase is monitored.

### 2.3. Relating sensitivity to bioavailability

Previous studies have described bioavailability by comparing a characteristic mass transfer rate coefficient to a characteristic biodegradation rate coefficient (e.g., [14,15,19,85]). Relating these coefficients allows a quick assessment of which processes limit the overall contaminant removal. Since model sensitivities depend on the limiting process, this approach can also be useful in quantitatively evaluating the appropriate model complexity for a given system. The characteristic rate coefficients for biodegradation ( $\alpha_{\text{bio}}$ ) and mass transfer ( $\alpha_{\text{mt}}$ ) can be defined as

$$\alpha_{\text{bio}} = \frac{r_{\text{bio}}(t)}{C_1(t)} \quad (25)$$

$$\alpha_{\text{mt}} = \frac{15D_p}{a^2\bar{R}_2(t)} \quad (26)$$

where  $\bar{R}_2$  is the average retardation factor in Region 2. In most discussions of bioavailability, the characteristic rate coefficients are taken to be constant in time. This is true only if the system is governed by linear, first-order processes such as at very low concentrations and a constant biomass. If the biodegradation is represented using a Monod model, however, the value of  $\alpha_{\text{bio}}$  can change with time because of concentration changes and biomass growth or decay. When cometabolism and competitive inhibition are accounted for, the value of  $\alpha_{\text{bio}}$  will also be influenced by the concentration and biodegradation rate of the co-solute. If a nonlinear sorption isotherm model applies, the extent of solute retardation in Region

2 changes with the solute concentration and leads to a time-dependent  $\alpha_{\text{mt}}$ . Consequently, the time dependence of the characteristic rate coefficients should be considered for systems that require more complex models.

In this study, the rate coefficients are compared by plotting, for a given system condition and for a given point in time, the value of  $\alpha_{\text{mt}}$  against the value of  $\alpha_{\text{bio}}$ . These “bioavailability plots” of  $\alpha_{\text{mt}}$  versus  $\alpha_{\text{bio}}$  are created for the four base case studies: Type 1 soil, fast biodegradation (T1 F), Type 1 soil, slow biodegradation (T1 S), Type 2 soil, fast biodegradation (T2 F), and Type 2 soil, slow biodegradation (T2 S). Two model combinations are used for this analysis: diffusive mass transfer, nonlinear sorption, Monod biodegradation (D–N–M) and diffusive mass transfer, nonlinear-competitive sorption, Monod with co-solute biodegradation (D–Nc–Mc).

## 3. Results

The  $M/M_0$  for the first 10 days of the model simulations are shown for toluene in Fig. 2 and for TCE in Fig. 3. Corresponding graphs for bulk aqueous phase concentrations,  $C_w/C_{w0}$ , are given in Figs. 4 and 5. Similar graphs for the “Type r” soils are shown in Fig. 6 ( $M/M_0$ ) and Fig. 7 ( $C_w/C_{w0}$ ). Although model simulations were conducted for more than the 10 day period, the 10 day window shown in the graphs adequately displays the asymptotic trends without suppressing the early time behavior of the different simulations. The graphs in each figure are organized to show the results of the low  $M_0$  simulations in the left column and the results of the high  $M_0$  simulations in the right column. The graphs are also organized to show a general increase in the disparity between the simulation results for the several model combinations from the upper left graph (most similar) to the lower right graph (most dissimilar), that is, from the low  $M_0$ , Type 1 soil, fast biodegradation rate scenario (T1 F) to the high  $M_0$ , Type 2 soil, slow biodegradation rate scenario (T2 S). In Figs. 2–7, the abbreviations from Fig. 1 are used to designate each model formulation. The “\*” symbols in place of a model formulation abbreviation indicates that the results are insensitive to that component of the model formulation.

The “bioavailability plots” of  $\alpha_{\text{mt}}$  versus  $\alpha_{\text{bio}}$  are shown in Fig. 8, with the results for toluene in the top graph and the results for TCE in the bottom graph. The time dependence of  $\alpha_{\text{mt}}$  and  $\alpha_{\text{bio}}$  is illustrated by plotting points at 11 times, first at 0.25 day and then at daily time increments from day 1 to day 10. The plotted points for the D–Nc–Mc model (solid symbols in Fig. 8) and the D–N–M model (open symbols) on the same graph allow an evaluation of how the consideration of co-solutes influences the rate coefficients. The dotted lines in the graphs denote where  $\alpha_{\text{mt}} = \alpha_{\text{bio}}$ .

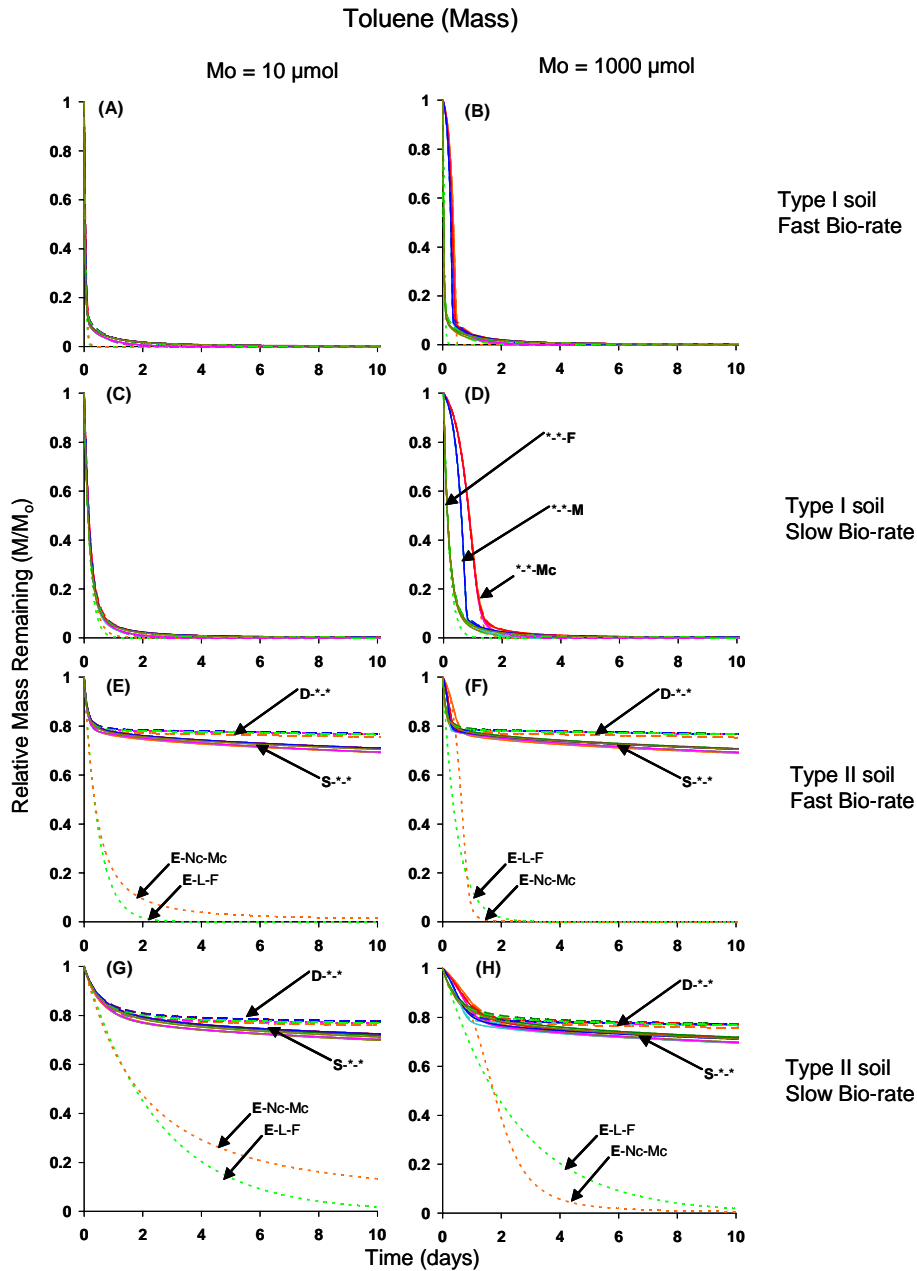


Fig. 2. Relative mass remaining ( $M/M_0$ ) with time for toluene in model simulations of the eight soil type, biodegradation rate (bio-rate), and  $M_0$  scenarios.

#### 4. Discussion

The sensitivity of the simulations' results to different representations of sorption, mass transfer, biodegradation, and the accounting for co-solutes depends on numerous factors. The following sections discuss the model sensitivities in the context of the factors explored in the case studies.

##### 4.1. Sensitivity to $M_0$

The effect of  $M_0$  is most pronounced in the Type 1 soil where sorption and mass transfer constraints are

minimal (Fig. 2A–D and Fig. 3A–D). The differences between modeling results are less apparent for the low  $M_0$  scenarios. Results for toluene show little difference between the low  $M_0$  simulations for the Type 1, fast and Type 1, slow biodegradation cases (Fig. 2A and C). There is similar agreement in model results for TCE at low  $M_0$  in the Type 1, fast and Type 1, slow cases (Fig. 3A and C). The better agreement among models at the lower  $M_0$  is intuitive based on examination of Eqs. (15)–(17), which approach the form of first-order biodegradation (Eq. (24)) as  $C_w$  becomes smaller. In addition, the influence of competitive inhibition is also larger in the high  $M_0$  cases (see Eqs. (17) and (18)).

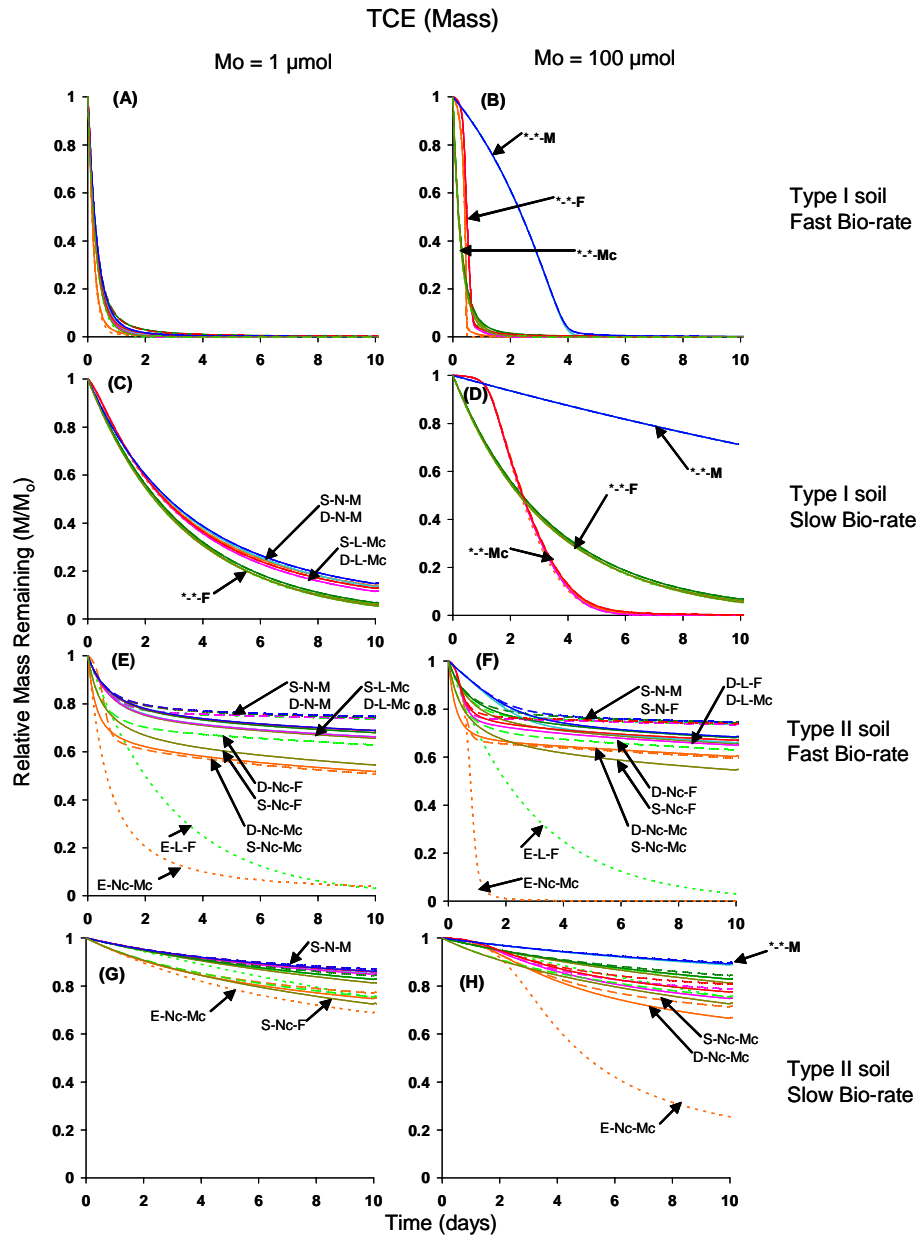


Fig. 3. Relative mass remaining ( $M/M_0$ ) with time for TCE in model simulations of the eight soil type, biodegradation rate (bio-rate), and  $M_0$  scenarios.

The biodegradation components of the different models again converge at later times when  $C_w$  decreases and inhibition becomes less important. These results illustrate the importance of considering the solute concentrations when selecting the most appropriate model. In particular, at the beginning of remediation periods, when solute concentrations are at a maximum, the commonly applied first-order biodegradation kinetics may oversimplify the degradation process—even for a single solute system. At longer remediation periods (as solute mass is depleted), however, the need for a more complex biodegradation model is relaxed so that a first-order biodegradation model may be appropriately assumed.

#### 4.2. Sensitivity to biodegradation rate

Slower biodegradation rates augment the differences in the representation of biodegradation and the effect of  $M_0$ . The increased differences among models for the slower biodegradation rates result from slower mass removal and the concomitant longer periods of higher concentrations that exaggerate the effects of self-inhibition (i.e., substrate saturation) and competitive inhibition. This is particularly true for the Type 1 soils where the biodegradation rates, rather than the mass transfer rates, control the overall mass removal. (Note the distinct grouping of models by the biodegradation

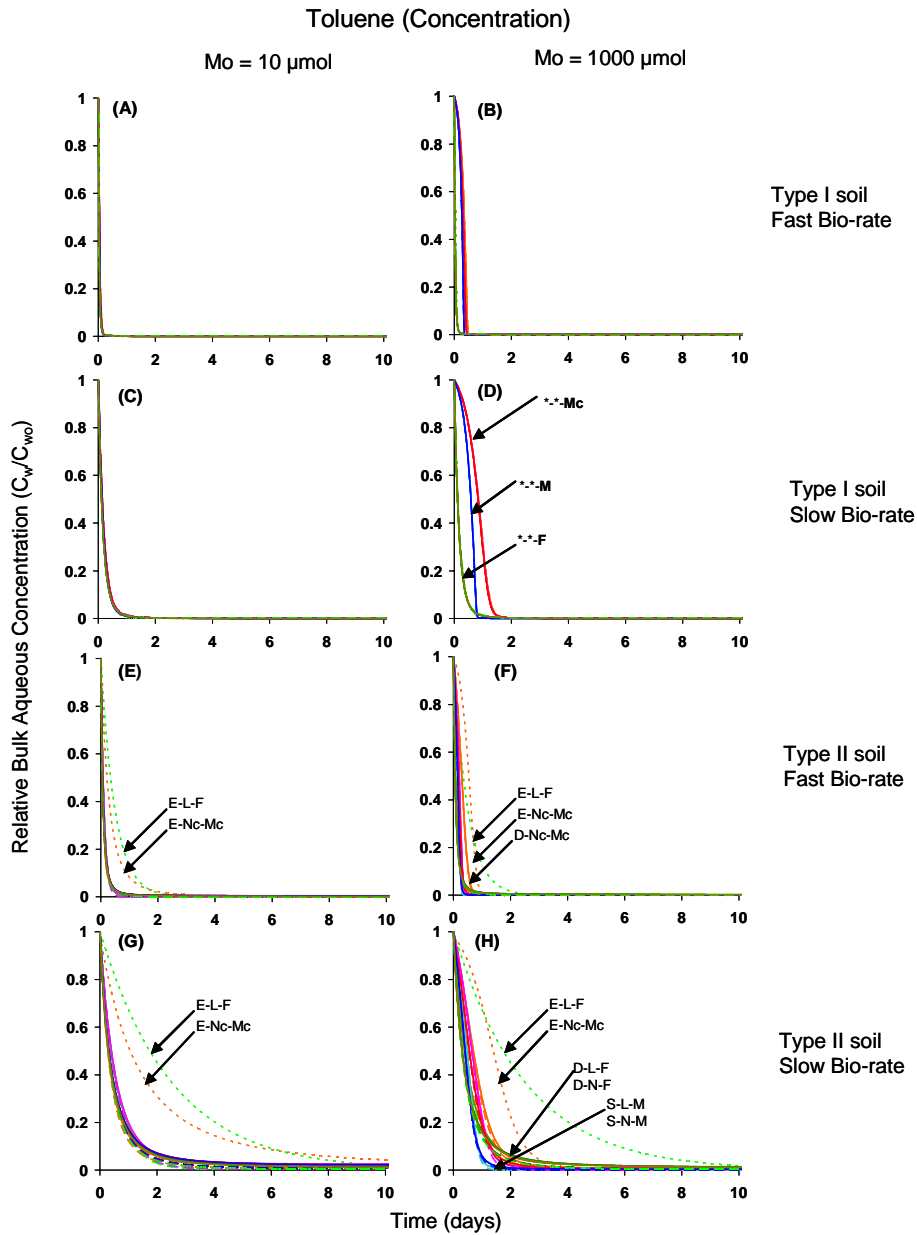


Fig. 4. Relative bulk aqueous phase concentration ( $C_w/C_{w0}$ ) with time for toluene in model simulations of the eight soil type, biodegradation rate (bio-rate), and  $M_0$  scenarios.

component that is most apparent in Fig. 2D and Fig. 3D.)

### 4.3. Sensitivity to soil type (sorption/mass transfer constraints)

#### 4.3.1. Type 1 and Type 2 soils

The different sorption and mass transfer constraints of the two soil types greatly influence model compatibility. In the Type 1 soil (lower sorption strength and faster mass transfer rates) modeling results are fairly uniform for toluene (Fig. 2A–D). In particular, low sorption affinities and rapid mass transfer rates decrease the sen-

sitivity to the representation of sorption and mass transfer relative to the representation of biodegradation. The lower sorption and mass transfer constraints in the Type 1 soil, however, result in greater sensitivity to the biodegradation component, thus the more pronounced effect of  $M_0$  and the grouping by biodegradation representation in the Type 1 soil. For toluene and TCE, the first-order biodegradation models (\*-\*-F), which do not account for inhibition and toxicity effects, generally show the most rapid mass removal, especially at early times. For toluene, single-substrate Monod models (\*-\*-M), which do account for enzyme affinity and substrate saturation but not competitive inhibition

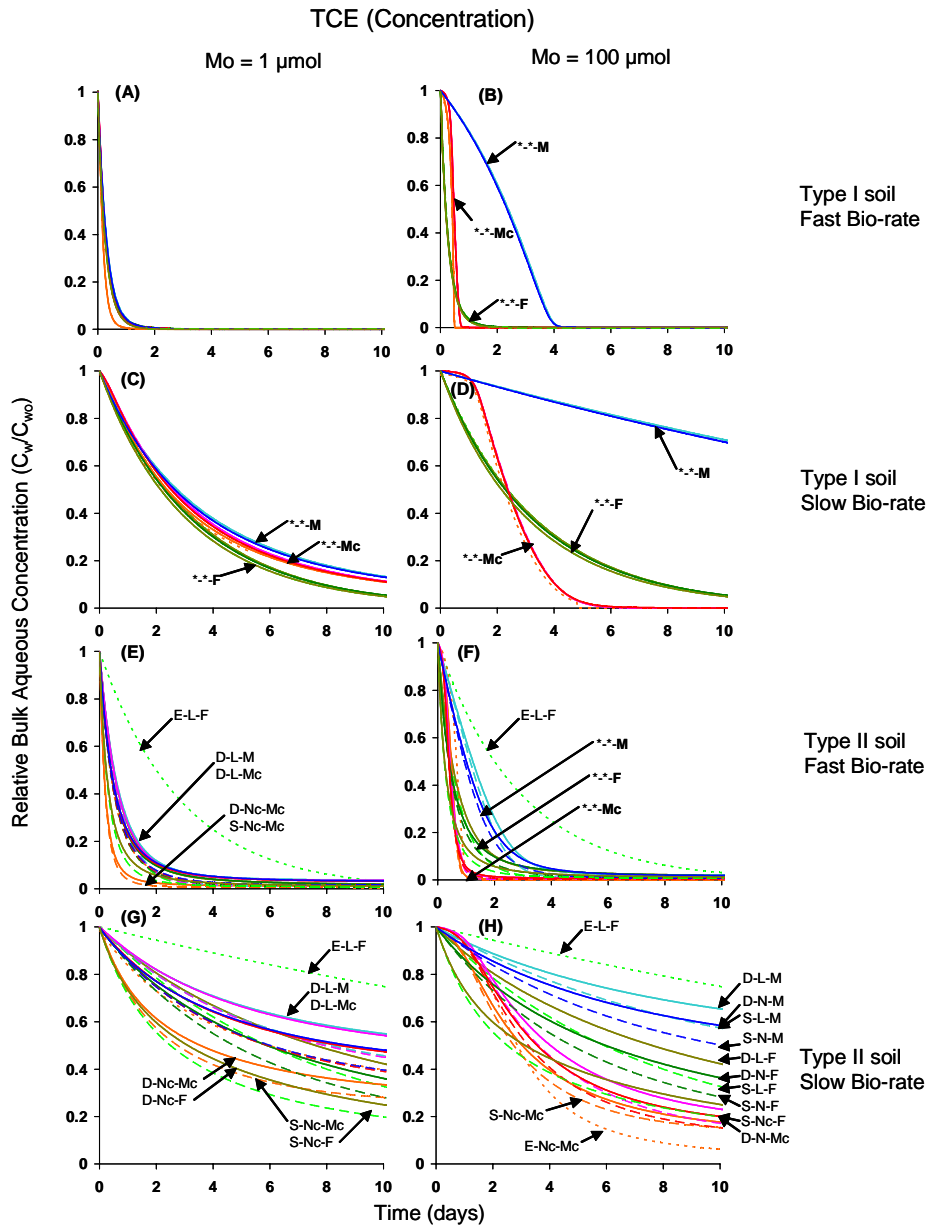


Fig. 5. Relative bulk aqueous phase concentration ( $C_w/C_{w0}$ ) with time for TCE in model simulations of the eight soil type, biodegradation rate (bio-rate), and  $M_0$  scenarios.

or product toxicity, have the second fastest mass removal, and cometabolic Monod models (\*-\*—Mc), which consider both enzyme affinity and co-solute effects, have the slowest removal. The grouping by the biodegradation component are the same for TCE, except that the cometabolic Monod models show faster mass removal than the single contaminant Monod models (Fig. 3A and D), a consequence of accounting for the enhancement of the TCE biodegradation rate due to the transformation yield on the biodegradation rate of toluene (Eq. (18)).

The Type 2 soil (higher sorption strength and slower mass transfer rates) shows the opposite grouping of models as the Type 1 soils; that is, by mass transfer rep-

resentation rather than by biodegradation representation (Fig. 2E–H and Fig. 3E–H). Also for the Type 2 soil, the discrepancies between the equilibrium, simple, and diffusion mass transfer models increase with time. The mass removal in all the simulations is initially rapid as solutes in the instantaneous sorption sites are immediately released to, then biodegraded in, the bulk aqueous phase. Following this rapid reduction of solute concentrations in the bulk aqueous phase, mass depletion in the two-region models is constrained by slow diffusion of solute from the intraparticle region. When the potential biodegradation rate is faster than the rate at which solute is transferred from the intraparticle region, the concentrations in the bulk aqueous phase reach a

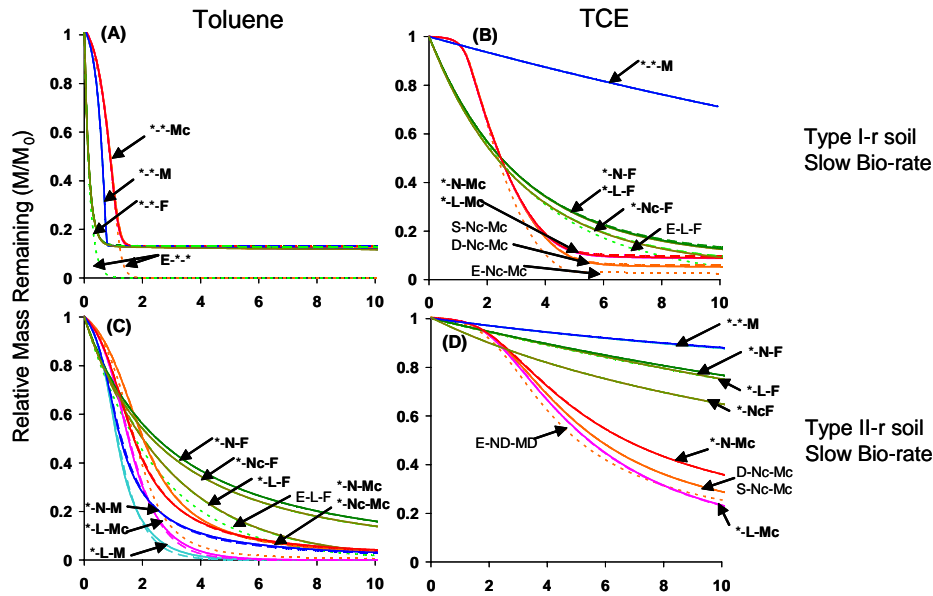


Fig. 6. Relative mass remaining ( $M/M_0$ ) with time for toluene (A, C) and TCE (B, D) for model simulations of the Type 1-r and Type 2-r soils and slow biodegradation rate (bio-rate). All simulations are conducted for the high  $M_0$  scenarios (toluene = 1000  $\mu\text{mol}$  and TCE = 100  $\mu\text{mol}$ ).

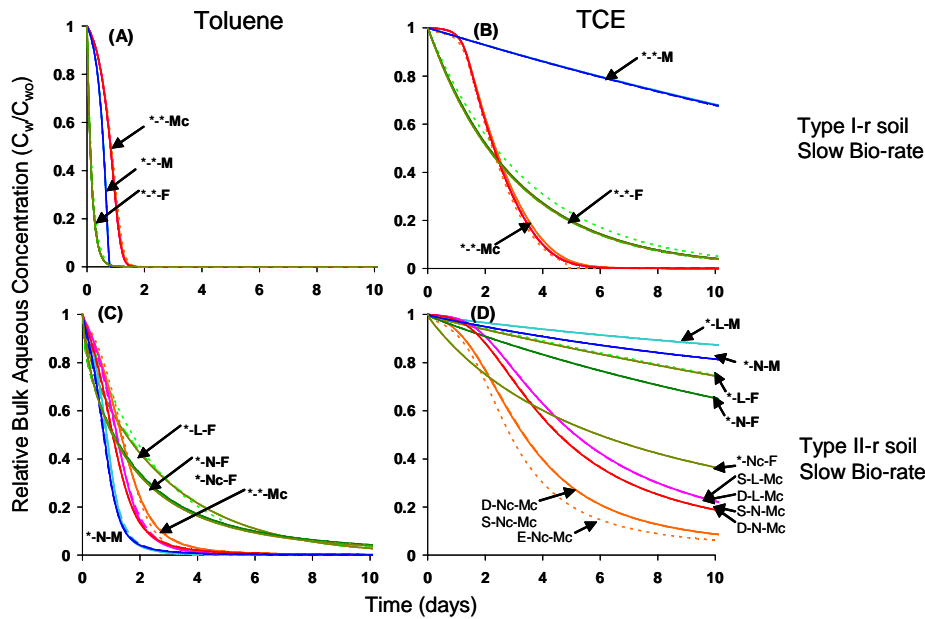


Fig. 7. Relative bulk aqueous phase concentration ( $C_w/C_{w0}$ ) with time for toluene (A, C) and TCE (B, D) for model simulations of the Type 1-r and Type 2-r soils and slow biodegradation rate (bio-rate). All simulations are conducted for the high  $M_0$  scenarios (toluene = 1000  $\mu\text{mol}$  and TCE = 100  $\mu\text{mol}$ ).

low steady-state value (Fig. 4E–H), the inter-region concentration gradient for mass transfer remains nearly constant, and there is a nearly linear mass removal with time (Fig. 2E–H). The equilibrium model, which assumes no mass transfer constraints, shows the most rapid mass removal. The slower mass removals observed for the simple mass transfer model as compared to the diffusion model result from equating the first-order mass transfer rate to the asymptotic mass transfer rate of the

diffusion model (see Eq. (23)). The bias of assuming the simple mass transfer model would be in the opposite direction (i.e., toward optimistic removal) had a diffusion rate been chosen from an earlier time (e.g., if it were based on a short-term desorption study or early field results).

The Type 2 soil also exhibits a secondary sensitivity to the sorption component. Initially, when aqueous concentrations are nearer the equilibrium points used

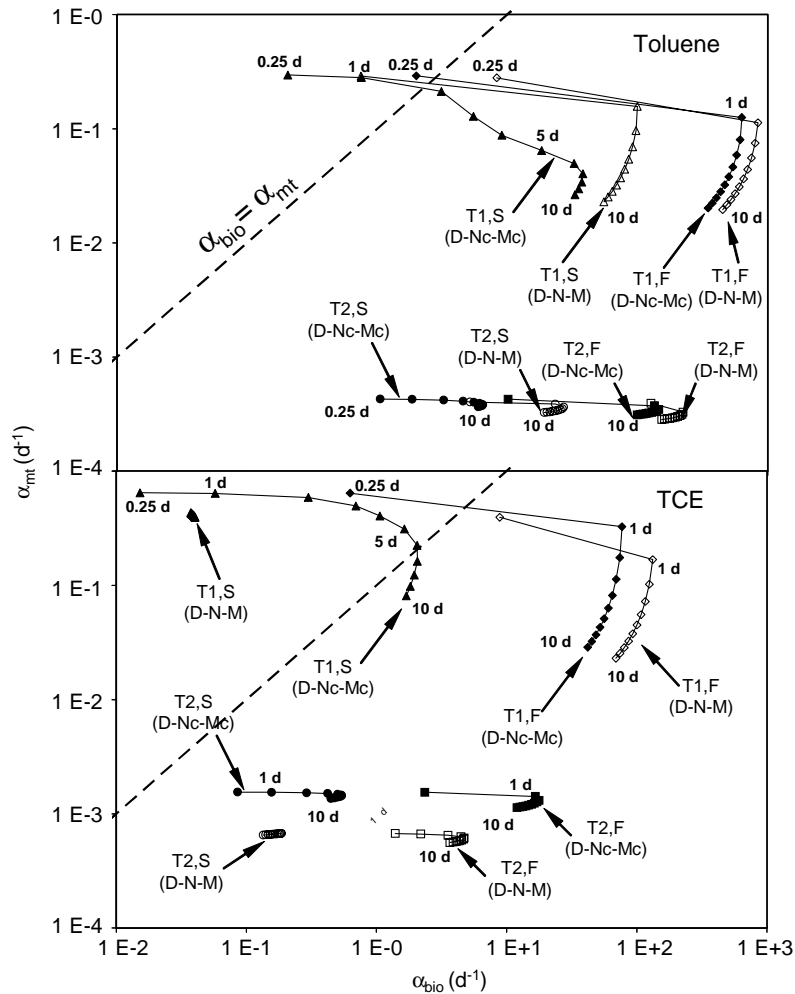


Fig. 8. Bioavailability plots showing the characteristic rate coefficients for mass transfer ( $\alpha_{mt}$ ) versus biodegradation ( $\alpha_{bio}$ ) for toluene and TCE. Comparison is made using the D–N–M and D–Nc–Mc models at time = 0.25 day, then at increments of 1 day from time = 1 day to time = 10 days. The alpha-numeric symbols designate the modeling scenario (e.g., T1 F = Type 1 soil, fast biodegradation rate). The dotted lines denote where  $\alpha_{mt} = \alpha_{bio}$ .

to relate the linear and nonlinear isotherms, the nonlinear sorption models have mass removal rates similar to their linear model counterparts (Fig. 2E–H and Fig. 3E–H). As the aqueous concentrations become small, however, the nonlinear sorption models have greater sorption affinity, resulting in slower diffusion/desorption rates and prolonged mass removal times compared to their linear counterparts (see especially Fig. 3E and F).

#### 4.3.2. Type 1-r and Type 2-r soils

The scenarios with low sorption capacity coupled with slow mass transfer rates (Type 1-r soil) and high sorption capacity coupled with rapid mass transfer rates (Type 2-r soil) are shown in Fig. 6 ( $M/M_0$ ) and Fig. 7 ( $C_w/C_{w0}$ ). The mass removal for the Type 1-r soil is similar to the Type 1 soil during early times, with results grouped based on the models biodegradation component (Fig. 6A and B). After this initial period, results from all models converge (except the equilibrium mod-

els, which are unaffected by changes in mass transfer constraints) as slow mass transfer limits solute bioavailability. Because toluene has faster biodegradation rates than TCE, the effect of the slower mass transfer rate is most evident for toluene (Fig. 6A). Although not clearly apparent in the 10 day window shown, results begin to diverge in the later times based on the model's mass transfer component. Thus for the case of low sorption capacity yet slow mass transfer rates, an accurate representation of both biodegradation and mass transfer is needed to adequately simulate the full  $M/M_0$  profile, while results are less sensitive to the sorption component of the models. Interestingly, the  $C_w/C_{w0}$  perspective shows little differences between the Type 1 and the Type 1-r soils (compare Fig. 4D and Fig. 7A), illustrating that observations based on only the concentration perspective cannot readily display the effects of mass transfer (see below for further discussion of this topic).

The Type 2-r soil (high sorption capacity and a rapid mass transfer rate) also displays two groupings of simulation results (Fig. 6C and D). First, results for scenarios with rapid mass transfer rates and slow biodegradation rates are grouped based on the model's representation of biodegradation. These groupings are similar to that discussed above in the section on sensitivity and biodegradation rate. The second grouping is by the representation of sorption, which in the Type 2-r soil is the dominant process limiting bioavailability. The differences between the linear, nonlinear, and nonlinear-competitive sorption models are initially negligible, but mass removal rates for the nonlinear sorption models become increasingly slower than the linear models, reflective of the greater sorption strength at lower solute concentrations. The nonlinear-competitive sorption models follow the same trends as the nonlinear models except for slightly greater mass removal, indicative of the reduced sorption capacity (increased bioavailability) due to the competitive sorption between toluene and TCE. An exception to this general observation is the behavior of the competitive sorption and cometabolic biodegradation models for toluene (Fig. 6C). Mass removal rates for the \*–Nc–Mc models are actually less than the other cometabolic biodegradation models. This anomaly is caused by the increased aqueous concentration of TCE in the \*–Nc–Mc models that inhibits the mass removal of toluene and slows the biomass growth because of greater product toxicity.

#### 4.4. Sensitivity to primary substrate vs. cometabolite

The differences among modeling results are more prominent for TCE mass removal than for toluene mass removal (e.g., compare Fig. 2D with Fig. 3D). For toluene, the first-order and single-substrate Monod biodegradation models give similar mass removal rates as the cometabolic Monod model for several scenarios. In contrast, for TCE, the first-order and single-substrate Monod biodegradation models are only comparable to the cometabolic Monod model in the Type 1, low  $M_0$  scenarios (Fig. 3A and C). The sorption and mass transfer of toluene and TCE are not sufficiently dissimilar to account for their different sensitivities. Rather, the greater sensitivity among the models for TCE is caused by at least two factors. First, as discussed previously, the slower biodegradation rates for TCE tend to augment model sensitivities to the biodegradation component. Second, the TCE biodegradation rates in the cometabolic Monod models are linked to the biodegradation rates of toluene (see Eq. (18)). Thus the sensitivities in the cometabolic Monod model for toluene are compounded in the cometabolic model for TCE. The greater sensitivity in modeling TCE is likely general to all cometabolites because biodegradation rate parameters for cometabolic substances are generally orders of magni-

tude lower than those of their primary growth substrates [7].

#### 4.5. Sensitivity to total mass vs. aqueous concentration

The results shown as  $C_w/C_{w0}$  (Figs. 3 and 4) are more similar than the corresponding results shown as  $M/M_0$  (Figs. 1 and 2). This is especially true when biodegradation rates are fast and mass transfer rates are slow. For these scenarios, bulk aqueous concentrations are rapidly depleted to very low values for all model types, even though the prediction of contaminant mass removal may vary among models (e.g., compare Fig. 2E–F with Fig. 3E–F). When  $C_w/C_{w0}$  is the evaluation criteria, even the E–L–F model performs similar to the more complex models for many scenarios. Hence, the appropriateness of model assumptions not only depends on the physical–biological properties of the subsurface environment, but also on the evaluation criteria. The need for a more sophisticated model is relaxed when only bulk aqueous phase concentrations are of concern.

Another interesting comparison between  $M/M_0$  and  $C_w/C_{w0}$  perspectives is the differences in the relative removal rates between the equilibrium (E), simple (S), and diffusion (D) models. For the  $M/M_0$  perspective, the equilibrium models consistently show the greatest removals, and the simple mass transfer models have the lowest removals. (Recall that the lower mass removals for the simple mass transfer models are due to matching the first-order mass transfer rate coefficients to the asymptotic diffusion rates.) The  $C_w/C_{w0}$  perspective shows an opposite trend; i.e., equilibrium models giving the lowest contaminant reductions and simple mass transfer models showing the greatest reductions. This apparent reversal in predictions of relative reductions demonstrates a potential fallacy of interpreting concentration reduction as mass removal. The  $C_w/C_{w0}$  perspective does not distinguish aqueous phase concentration reductions due to mass removal from concentration reduction due to contaminant sequestration into the immobile region. Thus, when mass transfer rates are small compared to biodegradation rates, contaminant concentrations in the bulk aqueous phase will quickly become low, although total contaminant mass removal is actually very slow. That total mass may not be properly modeled is irrelevant if the only criterion is aqueous phase concentrations (as might be the case for a flux-based standard). Often, however, there is also concern for long-term conditions under which aqueous phase biodegradation might no longer continue to occur (as in cases where the primary substrate is completely exhausted and biomass die-off occurs). In this situation, the total contaminant mass must be known and what was projected to be a “conservative” model under a  $C_w/C_{w0}$  criteria, may over-predict the actual contaminant removal.

#### 4.6. Interpreting model sensitivity using bioavailability plots

The bioavailability plots (Fig. 8) help interpret how model sensitivity changes for different case studies. The plots can be conceptually divided into four quadrants. Though the boundary values designating each quadrant are ambiguous, the lower right quadrant designates a mass transfer rate constrained system (low  $\alpha_{mt}$ , high  $\alpha_{bio}$ ), the upper left a biodegradation rate constrained system with (low  $\alpha_{bio}$ , high  $\alpha_{mt}$ ), the lower left a system with both mass transfer and biodegradation constraints, and the upper right a system with little or no constraints to solute mass removal. Each of the four combinations of soil type and biodegradation rate lay in a different quadrant of Fig. 8, reflecting the relative value of its bioavailability and sensitivity characteristics. The T1 F case, least sensitive to biodegradation and sorption/mass transfer representation, is in the upper left of the plots; the T1 S case, more sensitive to biodegradation, yet insensitive to sorption/mass transfer, is in the upper right; the T2 F case, more sensitive to sorption/mass transfer, yet relatively less sensitive to biodegradation, is in the lower right; and the T2 S case, relatively sensitive to both sorption/mass transfer and to biodegradation, is in the lower left. Such bioavailability plots are thus useful for providing a relative assessment of how sensitive different modeling scenarios are to their sorption, mass transfer, and biodegradation components. The specific values of parameters that demarcate the region into which any given scenario will fall, however, are still not well understood and will need further refinement through additional numerical and experimental studies. A four-region approach to defining bioavailability similar to that shown in Fig. 8 was also advocated in work by [15]. These authors prepared a figure that compared two experimentally measured, time-specific indices of the biotransformation potential and desorbed amount.

Fig. 8 also illustrates the effects of time dependence and co-solutes on  $\alpha_{mt}$  and  $\alpha_{bio}$ . In general,  $\alpha_{bio}$  dramatically increases over the course of the first day of the simulation (between 0.25 day and 1 day). This increase is attributed to the rapid growth of the biomass at early times. As solute concentrations diminish, the biomass growth decreases until there is net biomass decay, which reduces the value of  $\alpha_{bio}$  in the final days of the simulations. The value of  $\alpha_{mt}$  continuously decreases during the simulations because lower concentrations in the immobile domain lead to a rise in the sorption strength and a corresponding decrease in the pore diffusion rate. The decrease in  $\alpha_{mt}$  values with time would not occur for scenarios with linear sorption isotherms because pore diffusion rates are not concentration dependent. Because the lowest  $\alpha_{bio}$  values and greater  $\alpha_{mt}$  values are at the initial stages, the model simulations would be most sen-

sitive to the biodegradation component at early times and show increasing sensitivity to mass transfer at later times.

The co-solute effects on the  $\alpha_{bio}$  versus  $\alpha_{mt}$  values depend on the solute of interest. For toluene (primary substrate),  $\alpha_{mt}$  versus  $\alpha_{bio}$  values move toward the upper right between the D–N–M model and the D–Nc–Mc model due to the fact that co-solute inhibition reduced sorption in the presence of TCE. For TCE (cometabolite) the  $\alpha_{mt}$  versus  $\alpha_{bio}$  values usually move toward the upper left between the D–N–M and D–Nc–Mc models as a result of the increase in  $\alpha_{bio}$  for TCE in the presence of toluene. An exception to this trend is with the T1 F case, where the biodegradation rates for TCE are sufficiently rapid that toxicity effects of TCE degradation on the biomass growth become significant.

While many of the general characteristics of the  $\alpha_{mt}$  versus  $\alpha_{bio}$  plots of toluene and TCE are applicable to any single and/or co-solute system, some are solute specific. For example, both TCE and toluene rapidly biodegrade in aerobic conditions. This leads to large values of  $\alpha_{bio}$  so that the  $\alpha_{mt}$  versus  $\alpha_{bio}$  points are below the  $\alpha_{bio} = \alpha_{mt}$  line (dashed line in Fig. 8). Solutes with much slower biodegradation rates would plot in the biodegradation limited region (above the  $\alpha_{bio} = \alpha_{mt}$  line), and models for simulating these compounds would be more sensitive to the biodegradation component. In addition, mass removal times would be longer such that the time dependencies of  $\alpha_{bio}$  and  $\alpha_{mt}$  would be stretched across longer time scales. For the simulations with toluene and TCE, the changes in  $\alpha_{mt}$  versus  $\alpha_{bio}$  values (and thus model sensitivity) between the single solute model (D–N–M) and the co-solute model (D–Nc–Mc) are considerably less than the changes in  $\alpha_{mt}$  versus  $\alpha_{bio}$  values that arise because of differences in soil-type or biodegradation rate for the case studies that were chosen. This observation would likely change for other chemicals with different co-solute effects and different ranges of sorption, mass transfer, and/or biodegradation properties.

## 5. Conclusions

The simulations conducted here show that selection of an appropriate model cannot be separated from the biogeochemical context to which the model will be applied. In some cases, the formulation for modeling a given process can significantly effect short and/or long-term predictions. In other cases predictions are indifferent to the model selected. The relative sensitivity of predictions to model representations of sorption, mass transfer, biodegradation and the accounting for co-solute effects reflects which process controls mass removal. As found in previous studies and further substantiated in this work, modeling simplifications may be permissi-

ble for certain soil–water environments. For example, Scow and Hutson [66] and Simoni et al. [69] note that sorption and mass transfer limited systems can support the assumption of first-order biodegradation rates. As was further elucidated here, however, the modeling results for such systems will show more sensitivity to the representation of sorption, mass transfer, and also to co-solute effects on their abiotic processes. The reverse is also true: In environments with low sorption and mass transfer constraints, an equilibrium, linear sorption–desorption model may be sufficient, while a more complex biodegradation model component that accounts for cometabolism is needed to fully capture the system behavior. Models that simplify all components of sorption, mass transfer, and biodegradation are justified only when solute concentrations are relatively low and when all processes are rapid relative to the time scale of interest (such as the time of advection). This latter situation will be rare in the subsurface unless advection is impractically slow, and this is especially true for strongly sorbing contaminants and where a prediction of total mass removals (rather than only reductions in aqueous concentrations) is required.

The accounting for co-solute effects on one process will often increase the model sensitivity to other processes. For example, considering co-solute influences on sorption and mass transfer may necessitate a more complicated representation of biodegradation because competitive sorption often leads to reduced sorption and mass transfer constraints (faster desorption) and thus greater sensitivity to the biodegradation component. The dependency of the cometabolite degradation on the utilization of the primary growth substrate means that simulations of the cometabolism of a nongrowth substrate will have greater sensitivity to simplifications of the biodegradation component than will similar simulations for the primary growth substrate. In particular, this study shows that the use of first-order biodegradation rate models for a cometabolite may substantially deviate from more complex models, even in scenarios where a first-order model is justified for the primary growth substrate.

Bioavailability plots of a characteristic mass transfer rate coefficient ( $\alpha_{mt}$ ) versus a characteristic biodegradation rate coefficient ( $\alpha_{bio}$ ) are useful for assessing the relative sensitivities to model components and evaluating how bioavailability and sensitivity change with time. These plots show that biodegradation rates quickly increase at early times, while mass transfer rates for systems with nonlinear sorption decrease with time. As a result, model simulations will be most sensitive to the biodegradation component at early times and show increasing sensitivity to mass transfer at later times. Future work should more rigorously explore how modeling sensitivity is affecting the specific parameters of a given system and how these change over time. A remaining

challenge is to define how this sensitivity can be quantitatively measured and defined for real systems and for a wide range of solutes. Although it is expected that the results shown for these batch systems are valid for “volume elements” of field-scale systems, real systems will be of larger volume and show slower mass removal rates than the batch-scale simulations conducted here.

Finally, even though these simulations were couched in environmentally relevant scenarios and the models spanned a range of complexities, all models still simplified or neglected numerous process complexities that can influence contaminant persistence in the subsurface. Factors that were not explored here include both particle-scale heterogeneities (geometry, shape, internal sorption and pore structure) and large-scale heterogeneities (clay inclusions and preferential pathways). All such heterogeneities will add complexity to accurately representing sorption, mass transfer, and also the transport of oxygen and nutrients to zones of biomass growth. These factors will be particularly important in advective environments and under conditions where solutes transport at different rates. Nevertheless, the results presented in this study can help guide the selection of an appropriate level of model complexity for some systems and also serve as a more general basis for quantifying and discussing the factors influencing bioavailability and model sensitivity.

## Acknowledgements

Funding for this research has been supported by Agreement Number R828771-0-01 from the United States Environmental Protection Agency, Science to Achieve Results (STAR) program.

## References

- [1] Alagappan G, Cowan R. Substrate inhibition kinetics for toluene and benzene degrading pure cultures and a method for collection and analysis of respirometric data for strongly inhibited cultures. *Biotechnol Bioeng* 2003;83(7):798–809.
- [2] Allen-King RM, Grathwohl P, Ball WP. New modeling paradigms for the sorption of hydrophobic organic chemicals to heterogeneous carbonaceous matter in soils, sediments, and rocks. *Adv Water Resour* 2002;25:985–1016.
- [3] Alvarez-Cohen L. Application of methanotropic oxidations for the bioremediation of chlorinated organics. In: Murrel JC, Kelly DP, editors. *Microbial growth on C<sub>1</sub> compounds*. Washington, DC: American Society for Microbiology; 1993. p. 337–50.
- [4] Alvarez-Cohen L, McCarty PL. Effects of toxicity, aeration, and reductant supply on trichloroethylene transformation by a mixed methanotropic culture. *Appl Environ Microbiol* 1991;57:228–35.
- [5] Alvarez-Cohen L, McCarty PL. A cometabolic biotransformation model for halogenated aliphatic compounds exhibiting product toxicity. *Environ Sci Technol* 1991;25:1381–6.
- [6] Alvarez-Cohen L, Speitel Jr GE. Kinetics of aerobic cometabolism of chlorinated solvents. *Biodegradation* 2001;12:105–26.

- [7] Arp DJ, Yeager CM, Hyman MR. Molecular and cellular fundamentals of aerobic cometabolism of trichloroethylene. *Biodegradations* 2001;12:81–103.
- [8] Ball WP, Roberts PV. Long-term sorption of halogenated organic-chemicals by aquifer material. 1. Equilibrium. *Environ Sci Technol* 1991;25(7):1223–36.
- [9] Ball WP, Roberts PV. Long-term sorption of halogenated organic-chemicals by aquifer material. 2. Intraparticle diffusion. *Environ Sci Technol* 1991;25(7):1237–49.
- [10] Başıgaoglu HB, McCoy J, Ginn TR, Loge FJ, Deitrich JP. A diffusion limited sorption kinetics model with polydispersed particles of distinct shapes and sizes. *Adv Water Resour* 2002;25:755–72.
- [11] Bengtsson G, Carlsson C. Degradation of dissolved and sorbed 2,4-dichlorophenol in soil columns by suspended and sorbed bacteria. *Biodegradation* 2001;12:419–32.
- [12] Beran M. Hydrograph prediction—how much skill? *Hydrol Earth Syst Sci* 1999;3(2):305–37.
- [13] Beven K. Prophecy, reality and uncertainty in distributed hydrological modeling. *Adv Water Resour* 1993;16(1):41–551.
- [14] Bosma TN, Middeldorp PJM, Schraa G, Zehnder AJB. Mass transfer limitation of biotransformation: quantifying bioavailability. *Environ Sci Technol* 1997;31(1):248–52.
- [15] Braida WJ, White JC, Pignatello JJ. Indices for bioavailability and biotransformation potential of contaminants in soils. *Environ Toxicol Chem* 2004;23(7):1585–91.
- [16] Brusseau ML. The effect of nonlinear sorption on transformation of contaminants during transport in porous-media. *J Contam Hydrol* 1995;17(4):277–91.
- [17] Chang HL, Alvarez-Cohen L. Model of the cometabolic biodegradation of chlorinated organics. *Environ Sci Technol* 1995;29:2357–67.
- [18] Chen YM, Abriola LM, Alvarez PJJ, Anid PJ, Vogel TM. Modeling transport and biodegradation of benzene and toluene in a sandy aquifer material: comparisons with experimental results. *Water Resour Res* 1992;28(7):1833–47.
- [19] Chung G, McCoy BJ, Scow KM. Criteria to assess when biodegradation is kinetically limited by intraparticle diffusion and sorption. *Biotechnol Bioeng* 1993;41(6):6258–632.
- [20] Coats KH, Smith BD. Dead-end pore volumes and dispersion in porous media. *Soc Pet Eng J* 1964;4:73–84.
- [21] Copeland RA. *Enzymes: a practical introduction to structure, mechanism, and data analysis*. New York, NY: VCH Publishers, Inc.; 1996.
- [22] Connaughton DF, Stedinger JR, Lion LW, Shuler MI. Description of time-varying desorption-kinetics—release of naphthalene from contaminated soils. *Environ Sci Technol* 1993;27(12):2397–403.
- [23] Cornelissen G, Gustafsson O. Sorption of phenanthrene to environmental black carbon in sediment with and without organic matter and native substrates. *Environ Sci Technol* 2004;38(1):148–55.
- [24] Cornelissen G, Rigterink H, Vrind BA, ten Hulscheren DTEM, Ferdinandy MMA, van Noort PCM. Two-stage desorption kinetics and in situ partitioning of hexachlorobenzene and dichlorobenzenes in a contaminated sediment. *Chemosphere* 1997;35(10):2405–16.
- [25] Crank J. *The mathematical of diffusion*. 2nd. ed. New York, NY: Oxford University Press, Inc.; 1975.
- [26] Criddle CS. The kinetics of cometabolism. *Biotechnol Bioeng* 1993;41(11):1048–56.
- [27] Crittenden JC, Luft P, Hand DW, Oravitz JL, Loper SW, Arl M. Prediction of multicomponent adsorption equilibria using ideal adsorbed solution theory. *Environ Sci Technol* 1985;19(11):1037–43.
- [28] Edwards VH. Influence of high substrate concentrations on microbial kinetics. *Biotechnol Bioeng* 1970;12(5):679.
- [29] El-Farhan YH, Scow KM, de Jonge LW, Rolston DE, Moldrup P. Coupling transport and biodegradation of toluene and trichloroethylene in unsaturated soils. *Water Resour Res* 1998;34(3):437–46.
- [30] Ely RL, Williamson KJ, Guenther RB, Hyman MR, Arp DJ. A cometabolic kinetics model incorporating enzyme inhibition, inactivation, and recovery: I. Model development, analysis, and testing. *Biotechnol Bioeng* 1995;46:218–31.
- [31] E.P.A. National primary drinking water regulations. Contaminant specific fact sheets (Technical Version). EPA 811-F-95-004-T. 1995.
- [32] Fry VA, Istok JD. Effects of rate-limited desorption of the feasibility of in situ bioremediation. *Water Resour Res* 1994;30(8):2413–22.
- [33] Gamst J, Moldrup P, Rolston DE, Scow KM, Hendriksen K, Komatsu T. Time-dependency of naphthalene sorption in soil: simple rate-, diffusion-, and isotherm-parameter-based models. *Soil Sci* 2004;169(5):342–54.
- [34] Gamst J, Olesen T, De Jonge H, Moldrup P, Rolston DE. Non-singularity of naphthalene sorption in soil: observations and the two-compartment model. *Soil Sci Soc Am J* 2001;65:1622–33.
- [35] Gandhi RK, Hopkins GD, Goltz MN, Gorelick SM, McCarty PL. Full-scale demonstration of in situ cometabolic biodegradation of trichloroethylene in groundwater. 2. Comprehensive analysis of field data using reactive transport modeling. *Water Resour Res* 2002;38(4). Art. No. 1040.
- [36] Graber ER, Borisover M. Competitive sorption of organic contaminants. *J Contam Hydrol* 2003;67:159–75.
- [37] Griffioen J. Suitability of the first-order mass transfer concept for describing cyclic diffusive mass transfer in stagnant zones. *J Contam Hydrol* 1998;34:155–65.
- [38] Haggerty R, Harvey CF, von Schwerin CF, Meigs LC. What controls the apparent timescale of solute mass transfer in aquifers and soils? A comparison of experimental results. *Water Resour Res* 2004;40(1). Art. No. W01510.
- [39] Haggerty R, McKenna SA, Meigs LC. On the late-time behavior of tracer test breakthrough curves. *Water Resour Res* 2000;36(12):3467–79.
- [40] Harmon TC, Roberts PV. Comparison of intraparticle sorption and desorption rates for a halogenated alkene in a sandy aquifer material. *Environ Sci Technol* 1994;28(9):1650–60.
- [41] Hayduk W, Laudie H. Prediction of diffusion coefficients for non-electrolysis in dilute aqueous solutions. *Ind Eng Chem* 1974;58:19–27.
- [42] Hopmans JW, Šimůnek J. Review of inverse estimation of soil hydraulic properties. In: van Genuchten MT, Leij FJ, Wu L, editors. *Characterization and measurement of hydraulic properties of unsaturated porous media*. Riverside, CA: University of California; 1997. p. 643–60.
- [43] Huang W, Young TM, Schlautman MA, Yu H, Weber Jr WJ. A distributed reactivity model for sorption by soils and sediments. 9. General isotherm nonlinearity and applicability of the dual reactive domain model. *Environ Sci Technol* 1997;31(6):1703–10.
- [44] Huang W, Peng P, Yu Z, Fu J. Effects of organic matter heterogeneity on sorption and desorption of organic contaminants by soils and sediments. *Appl Geochem* 2003;18:955–72.
- [45] Johnson MD, Kienath II TM, Weber Jr WJ. A distributed reactivity model for sorption by soils and sediments. 14. Characterization and modeling of phenanthrene desorption rates. *Environ Sci Technol* 2001;35(8):1688–95.
- [46] Karapanagioti HK, Gossard CM, Strevett KA, Kolar RL, Sabatini DA. Model coupling intraparticle diffusion/sorption, nonlinear sorption, and biodegradation processes. *J Contam Hydrol* 2001;48:1–21.
- [47] Karickhoff SW. Semiempirical estimation of sorption of hydrophobic pollutants on natural sediments and soils. *Chemosphere* 1981;10(8):833–46.

- [48] Kim Y, Arp DJ, Semprini L. Kinetic and inhibition studies for the aerobic cometabolism of 1,1,1-trichloroethane, 1,1-dichloroethylene, and 1,1-dichloroethane by a butane-grown mixed culture. *Biotechnol Bioeng* 2002;80(5):498–508.
- [49] Kovárová-Kovar K, Egli T. Growth kinetics of suspended microbial cells: from single-substrate-controlled growth to mixed-substrate kinetics. *Microbiol Mol Biol Rev* 1998;62(3):646–66.
- [50] Ogram AV, Jessup RE, Ou LT, Rao PCS. Effects of sorption on biological degradation rates of (2,4-dichlorophenoxy) acetic acid in soils. *Appl Environ Microbiol* 1985;49(3):582–7.
- [51] Maraqa MA, Wallace RB, Voice TC. Effects of residence time and degree of water saturation on sorption nonequilibrium parameters. *J Contam Hydrol* 1999;36(1–2):53–72.
- [52] Martins JM, Mermoud A. Sorption and degradation of four nitroaromatic herbicides in mono and multi-solute saturated/unsaturated soil and batch systems. *J Contam Hydrol* 1998;33:187–210.
- [53] McCarty PL, Goltz MN, Hopkins GD, Dolan ME, Allan JP, Kawakami BT, et al. Full-scale evaluation of in situ cometabolic degradation of trichloroethylene in groundwater through toluene injection. *Environ Sci Technol* 1998;32(1):88–100.
- [54] McGinley PM, Katz LE, Weber Jr WJ. A distributed reactivity model for sorption by soils and sediments. 2. Multicomponent systems and competitive effects. *Environ Sci Technol* 1993;27(8):1524–31.
- [55] Monod J. The growth of bacterial cultures. *Ann Rev Microbiol* 1949;3:371–94.
- [56] Parker JC, Valocchi AJ. Conditions on the validity of equilibrium and first-order kinetic transport models in structured soils. *Water Resour Res* 1986;22(3):399–407.
- [57] Pedit JA, Miller CT. Heterogeneous sorption processes in subsurface systems. 1. Model formulations and applications. *Environ Sci Technol* 1994;28(12):2094–104.
- [58] Radke CJ, Prausnitz JM. Thermodynamics of multi-solute adsorption from dilute liquid solutions. *AIChE J* 1972;18:761–8.
- [59] Rao PSC, Jessup RE, Rolston DE, Davidson JM, Kilcrease DP. Experimental and mathematical-description of non-adsorbed solute transfer by diffusion in spherical aggregates. *Soil Sci Soc Am J* 1980;44(4):684–8.
- [60] Röling WFM, van Verseveld HW. Natural attenuation: what does the subsurface have in store? *Biodegradation* 2002;13:53–64.
- [61] Sabbah I, Ball WP, Young DF, Bouwer EJ. Misinterpretations in the modeling of contaminant desorption from environmental solids when equilibrium conditions are not fully understood. *Environ Eng Sci* 2005;22(3):350–66.
- [62] Schaefer CE, Schuth C, Werth CJ, Reinhard M. Binary desorption isotherms of TCE and PCE from silica gel and natural solids. *Environ Sci Technol* 2000;34(20):4341–7.
- [63] Schafer A, Bouwer EJ. Toluene induced cometabolism of *cis*-1,2-dichloroethylene and vinyl chloride under conditions expected downgradient of a permeable Fe(0) barrier. *Water Res* 2000;34(13):3391–9.
- [64] Schaerlaekens J, Mallants D, Simunek J, van Genuchten MT, Feyen J. Numerical simulation of transport and sequential biodegradation of chlorinated aliphatic hydrocarbons using CHAIN\_2D. *Hydrol Proc* 1999;16:2847–59.
- [65] Scow KM, Alexander M. Effect of diffusion on the kinetics of biodegradation—experimental results with synthetic aggregates. *Soil Sci Soc Am J* 1992;56(1):128–34.
- [66] Scow KM, Hutson J. Effect of diffusion and sorption on the kinetics of biodegradation: theoretical considerations. *Soil Sci Soc Am J* 1992;56:119–27.
- [67] Semprini L. Strategies for the aerobic cometabolism of chlorinated solvent. *Curr Opin Biotechnol* 1997;8:296–308.
- [68] Shonnard DR, Bell RL, Jackman AP. Effects of nonlinear sorption on the diffusion of benzene and dichloromethane from 2 air-dry soils. *Environ Sci Technol* 1993;27(3):457–66.
- [69] Simoni SF, Schäfer A, Harms H, Zender AJB. Factors affecting mass transfer limited biodegradation in saturated porous media. *J Contam Hydrol* 2001;50:99–120.
- [70] Šimůnek J, Jarvis N, van Genuchten MT, Gärdenäs A. Review and comparison of models for describing non-equilibrium and preferential flow and transport in the vadose zone. *J Hydrol* 2003;272:14–35.
- [71] Smith SC, Ainsworth CC, Traina SJ, Hicks RJ. Effect of sorption on the biodegradation of quinoline. *Soil Sci Soc Am J* 1992;56(3):737–46.
- [72] Sturman PJ, Stewart PS, Cunningham AB, Bouwer EJ, Wolfram JH. Engineering scale-up of in situ bioremediation processes: a review. *J Contam Hydrol* 1995;19:171–203.
- [73] ten Hulscher TEM, Vrind BA, van den Heuvel H, van der Velde LE, van Noort PCM, Beurskens JEM, et al. Triphasic desorption of highly resistant chlorobenzenes, polychlorinated biphenyls, and polycyclic aromatic hydrocarbons in field contaminated sediment. *Environ Sci Technol* 1999;33(1):126–32.
- [74] Tomida T, McCoy BJ. Polynomial profile approximation for intraparticle diffusion. *AIChE J* 1987;33(11):1908–11.
- [75] van Genuchten MT, Dalton FN. Models for simulating salt movement in aggregated field soils. *Geoderma* 1986;37(1–4):165–83.
- [76] van Genuchten MT, Wierenga PJ. Mass transfer studies in sorbing porous media. I. Analytical solutions. *Soil Sci Soc Am J* 1976;40(4):473–80.
- [77] Weber WJ, Huang WL, LeBoeuf EJ. Geosorbent organic matter and its relationship to the binding and sequestration of organic contaminants. *Colloid Surf A Physicochem Eng Aspect* 1999;151(1–2):167–79.
- [78] Weber WJ, McGinley PM, Katz LE. A distributed reactivity model for sorption by soils and sediments. 1. Conceptual basis and equilibrium assessments. *Environ Sci Technol* 1992;26(10):1955–62.
- [79] White JC, Pignatello JJ. Influence of bisolute competition on the desorption kinetics of polycyclic aromatic hydrocarbons. *Environ Sci Technol* 1999;33(23):4292–8.
- [80] Xia GS, Ball WP. Polanyi-based models for the competitive sorption of low-polarity organic contaminants on a natural sorbent. *Environ Sci Technol* 2000;34(7):1246–53.
- [81] Xing BS, Pignatello JJ, Gigliotti B. Competitive sorption between atrazine and other organic compounds in soils and model sorbents. *Environ Sci Technol* 1996;30(8):2432–40.
- [82] Young DF. Effects of experimental conditions on estimates of model parameters describing solute transport through porous media. PhD thesis. Johns Hopkins University, Baltimore, MD, USA. 1997.
- [83] Young DF, Ball WP. Effects of column conditions on the first-order rate modeling of nonequilibrium solute breakthrough. *Water Resources Res* 1995;31(9):2181–92.
- [84] Young DF, Ball WP. Two-region linear/nonlinear sorption modeling: batch and column experiments. *Environ Toxicol Chem* 1999;18(8):1686–93.
- [85] Zhang W, Bouwer EJ, Ball WP. Bioavailability of hydrophobic organic contaminants: effects and implications of sorption-related mass transfer. *Groundwater Monit Rev* 1998(Winter):126–38.